WBS 1.3 – Main Injector Upgrades

One focus of the Proton Plan is to increase beam intensity in the Main Injector by developing multi-batch slips tacking operation and increasing RF power for acceleration. The beam size will be larger resulting in unacceptably high losses in the injection and extraction regions unless apertures are increased. Radiation surveys of the Main Injector and beam loss studies indicate that the major sources of beam loss occur at injection, at transition and at extraction. Losses at transition are thought to be small compared to the injection and extraction losses. WBS elements 1.3.1 and 1.3.2 will increase the aperture in specific places and reduce beam tails to reduce these losses. Unavoidable losses due to stacking at injection need to be controlled so a Ring Collimation system will be designed and built.

The existing Beam Position Monitor system does not provide batch-by-batch information in NuMI multi-batch operation, and the Beam Loss Monitor system does not allow data-logging for an individual cycle. These instrumentation systems will be replaced as part of the Run II Upgrade Plan.

WBS 1.3.1 – Large Aperture Quadrupoles

With large batch intensities delivered from the Booster and particularly with the advent of slip stacking for NuMI that will result in increased longitudinal emittance, beam loss and activation become an issue in the Main Injector. The most critical locations for this loss are at the quadrupoles near each of the extraction transfer lines, specifically the NuMI, A1, P1, and abort extraction lines, and the transfer lines to and from the Recycler.

The aperture will be increased at these locations by replacing the present quadrupoles with large aperture WQB quadrupole magnets. A total of nine magnets were built including two spares. The MI acceptance at the Large Aperture locations is expected to increase by a factor of 2 from 40π to 80π by also moving the downstream Lambertsons 15 mm (Fig. 3.1.1) . All seven of the WQB magnets were installed during the Spring 06 shutdown but the Lambertsons were not moved. The acceptance increase is expected to increase by 50%. The expected aperture increase at the quad locations is about 10 mm (Fig. 3.1.2) and was verified by beam aperture scans (Fig. 3.1.3).

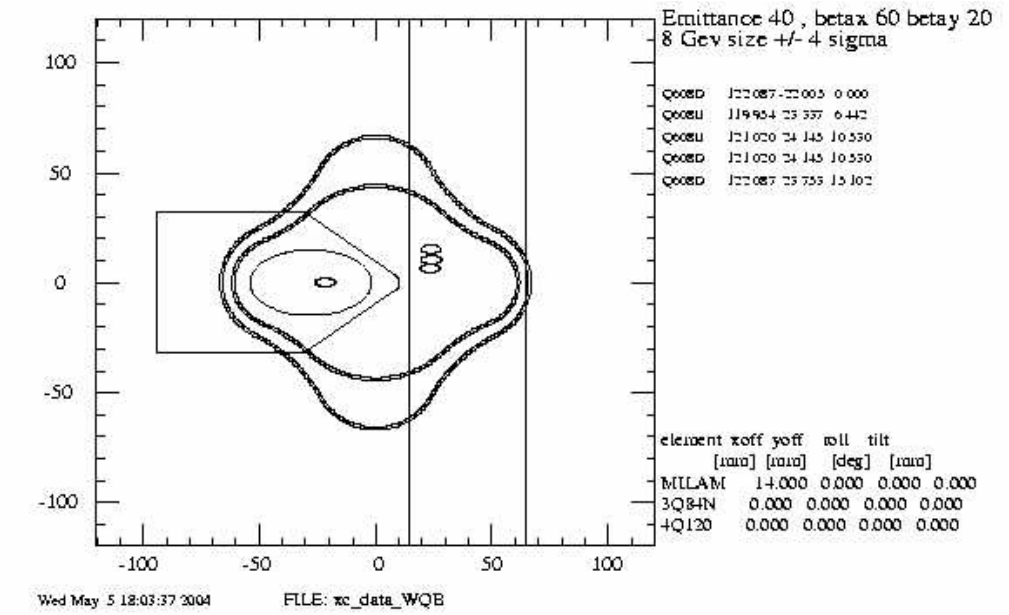

FIG 3.1.1: Present MI quadrupole and new WQB magnet apertures for the MI60 extraction region. Large ellipse shows the beam size at 8 GeV. Smaller ellipses are beam sizes at 120 GeV (circulating and extracted beams). Lambertson magnet apertures are also shown.

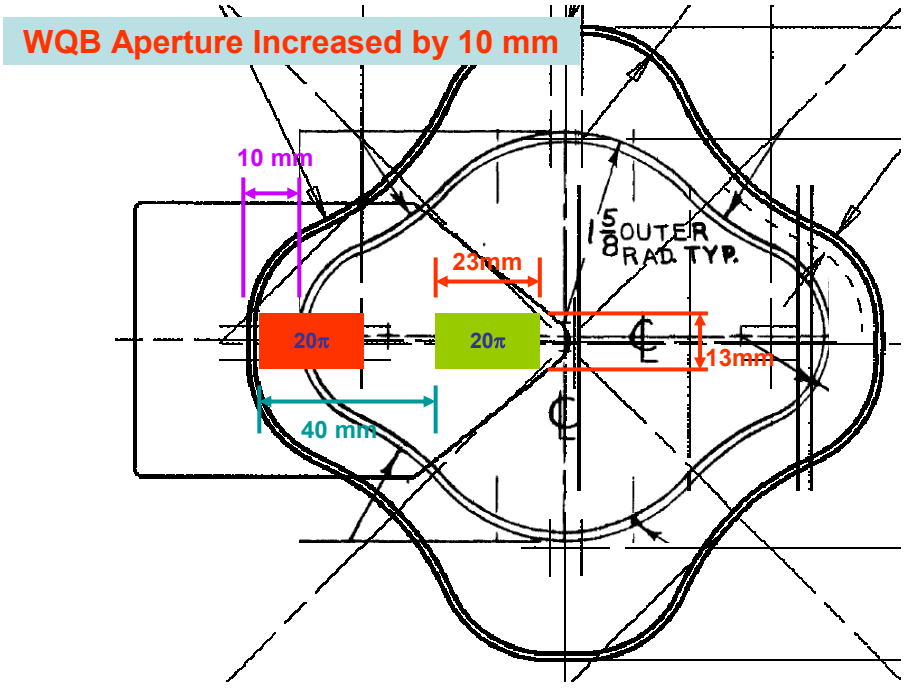

FIG 3.1.2: Schematic Illustrating the expected Aperture Increase from the WQB wide aperture quadrupole magnet.

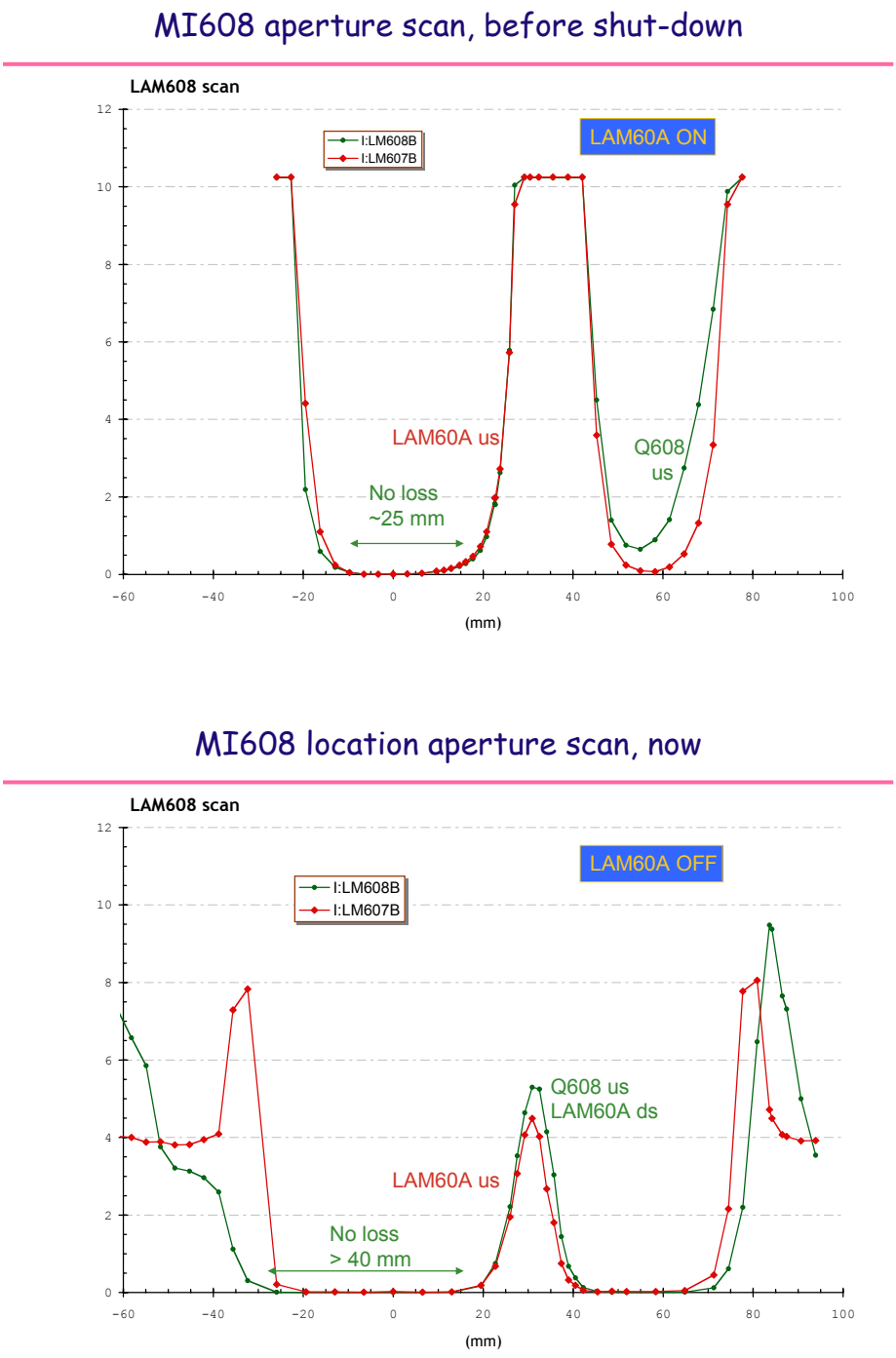

FIG 3.1.3: Aperture scans at the 608 Quad location before (top) and after (bottom) the installation of a WQB magnet. We can clearly see an aperture increase of around 15 mm as expected.

WBS 1.3.2 - Main Injector Collimation

The Main Injector Department has developed a program to monitor residual rates around the ring. The installation of a new Beam Loss Monitor (BLM) system under the auspices of the Run II Upgrade Plan will allow improved real-time monitoring. These studies activities are captured in WBS 1.3.2.1. Improved apertures, careful monitoring of input beam parameters and component moves and re-alignment, performed on an as needed basis during shutdowns, will help control the total beam loss in the Main Injector.

WBS 1.3.2 encompasses collimation systems to reduce the radiological impact of unavoidable beam loss. The most significant radiation issues are residual radiation induced in or near components that require maintenance and activation of materials outside of the tunnel where radioactive materials can be leached into water which will be pumped to the surface by sump pump systems. . Since there is little space in the Main Injector for collimators of any significant size, we have installed collimators in the MI-8 line to control the more significant injection losses. A collimator system will be installed in the Main Injector ring in the summer 2007 shutdown to help localize remaining losses. Design studies for this system have identified un-captured beam from slip-stacking injection as a component which can be collimated with high efficiency. Provisions for capturing beam lost by other mechanisms will be included in the plan. A review on June 30, 2006 recommended pursuit of a two stage (primary-secondary) collimation system (Fig. 3.2.1). We expect to install one or two thin tungsten primary collimators and several 20 ton steel secondary collimators. Significant study effort using the new BLM should permit the loss mechanisms to be further understood. Test collimators may be installed to enhance these loss study options.

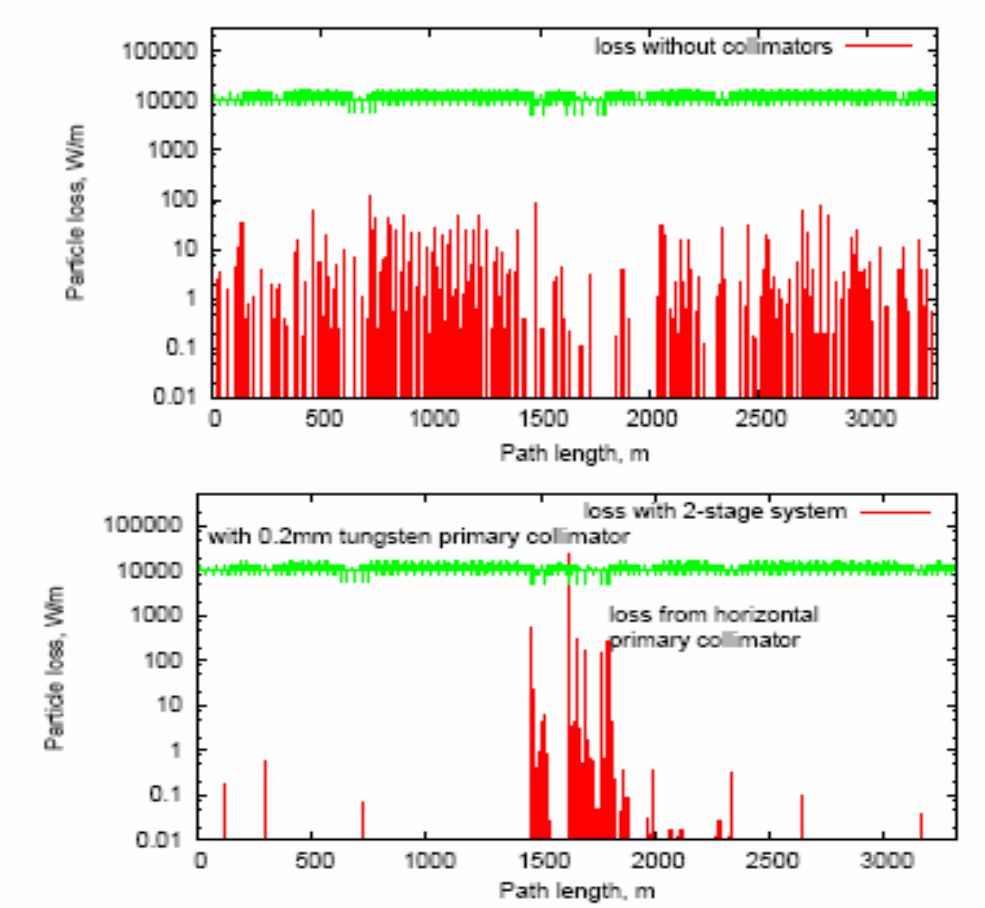

FIG 3.2.1: Losses in MI Tunnel without collimation (top) and with a two stage collimation system with one primary and 3 secondary collimators (bottom).

WBS 1.3.2.2 – MI-8 Collimator System Design & Commissioning

In expectation of increased beam intensity requirements associated with operation of the NuMI beamline, residual radiation around the Main Injector tunnel was examined prior to the 2004 Fermilab facility shutdown (see Residual Radiation Hints for Aperture and Alignment Issues in the Main Injector). We concluded that a small but significant contributor to the residual radiation was losses of beam due to tails of the Booster Beam which were not accelerated but were scraped around the Main Injector at locations which had only very little less aperture than other similar lattice locations. By providing a more defined beam from the Booster, we will reduce the losses from these tails which will reduce substantially the number of hot locations in the MI Ring. Collimation in the MI8 Line can provide this improved beam to the Main Injector. Tails from the Booster Beam may contribute residual radiation at other, as yet unidentified Main Injector locations.

A preliminary description for this work is available as MI8 Beamline Collimation Design (Beams-doc-1977). The design concept for this collimator system is based on the Booster beam collimation system. The difference between circulating and single pass beam collimation requires additional collimators. Table 3.2.1 compares the collimation requirements for circulating beam in the Booster and the one-pass beam in the MI8 transfer line.

Four collimators were installed in the MI8 line during the Spring 2006 Facility Shutdown. Two are in the 200" long space between magnets in the MI836 half-cell while the other two are in the similar location in the MI838 half cell about 90^{o} away in phase advance. Each collimator has a 2" x 2" aperture lined with 2 cm of stainless steel with a taper at the upstream end. The stainless steel channel is surrounded by steel shielding and marble. Each collimator is 45" long and has X and Y motion controls. The anticipated residual dose rate with a 1% beam loss is approximately 10 mrem/hr at 1 foot. The mechanical design is documented in Mechanical Design of MI8 Collimators (Beams-doc-2287). Radiation calculation and thermal calculation documents are in preparation and will be used to prepare radiation safety documents in preparation for system operation in Fall 2006.

Booster Collimators	**MI8 Collimators**
10 Hz at 5E12 Protons/pulse	10 Hz at 5E12 Protons/pulse
2% Loss at 8 GeV plus low energy loss	0.5% Loss at 8 GeV (or more)
Multi-turn circulating beam → collimators 1 Horizontal (radial outside) 1 Vertical (bottom)	One pass → collimators 4 Horizontal (inside, outside at two phases) 4 Vertical (top, bottom at two phases)
Tunnel not deep	Tunnel deep
Surface occupied	Surface not occupied
Air Activation not serious	Air Activation not serious
Ground water not an issue	Ground water not an issue

TABLE 3.2.1: Parameter comparison for the existing Booster collimator system and the proposed MI8 collimator system

FIG 3.2.2: Two of the four MI8 collimators in the MI8 tunnel.

WBS 1.3.3 – NuMI Multi-batch Operation

This WBS encompasses on-going work in the Main Injector to achieve multi-batch mixed mode operation. This work includes studies of extraction kicker rise and fall times, revised sequencer timing for NuMI, orbit studies of the NuMI extraction region, potential orbit distortions due to the NuMI Lambertson magnets, and slip stacking for NuMI.

The circumference of the Main Injector provides six "slots" for loading Booster batches. One slot is required for antiproton production, leaving five available for NuMI. Both programs will rely on schemes that allow more than one Booster batch to be loaded into a single slot. The baseline proposal is to use the technique called slip stacking that has been extensively developed for antiproton production. In this scheme, two batches are injected into the Main Injector at slightly different momenta, and therefore different velocities. This causes them to "slip" together, at which point they are captured by the RF. This allows two batches to be loaded into a single slot, at the cost of increased longitudinal emittance. Figure 3.3.1 illustrates slip stacking for antiproton production.

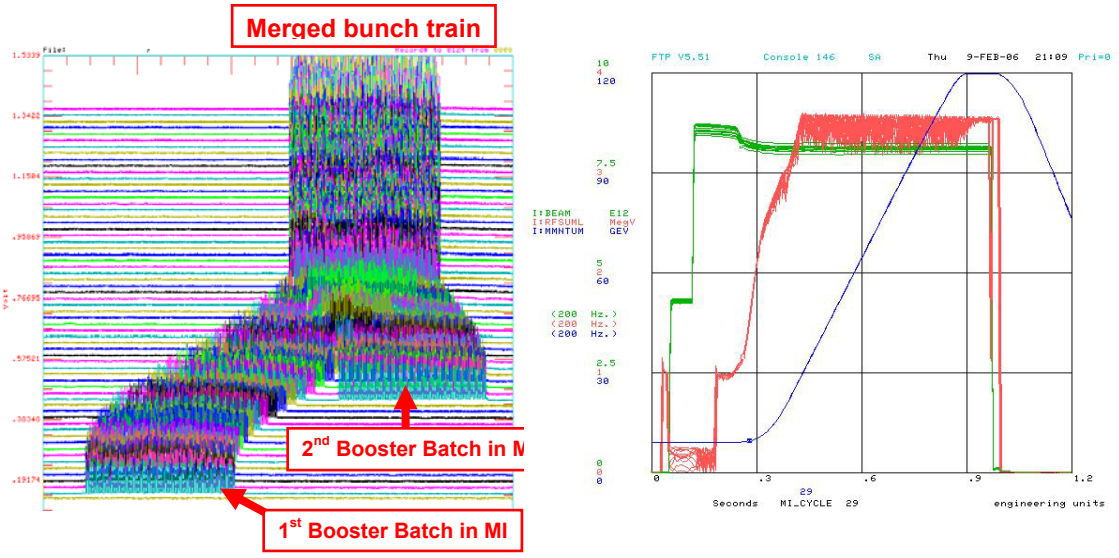

FIGURE 3.3.1: (Left) Mountain range picture showing merging of two Booster batches of protons in the Main Injector. The horizontal axis is the time for one orbit. The vertical axis is the number of orbits. (Right) Fast time plot during slip stacking – the green trace is the beam intensity (scale 0 to 8E12 protons), the red trace is the 53 MHz RF voltage and the blue curve shows the beam momentum for acceleration from 8 to 120 GeV.

During current operation, we slip stack two batches for antiproton production and then load five batches for NuMI, for a total of seven batches accelerated in the Main Injector. During 2005, the intensity was ramped to 2.35E13 for NuMI and 0.8E13 for pbar for a total of 3.15E13 particles per pulse.

The MI studies to develop slip stacking for NuMI operation started in February 2006. Under this scheme, it takes 12 Booster cycles to load and slip a total of 11 batches, two batches for antiproton production and nine for NuMI. The total intensity accelerated in the Main Injector can be then as high as 5.5E13 per cycle.

A schematic illustrating the slip stacking for NuMI and pbar production is shown in Fig. 3.3.2. A mountain range picture of real beam during multi-batch slip stacking is shown in Fig. 3.3.3 . The intensity of the multi-batched slip stacked beam during an MI study cycle is shown in Fig. 3.3.4. The estimated effort and time required for the development of slip stacking is based on the experience with antiproton production.

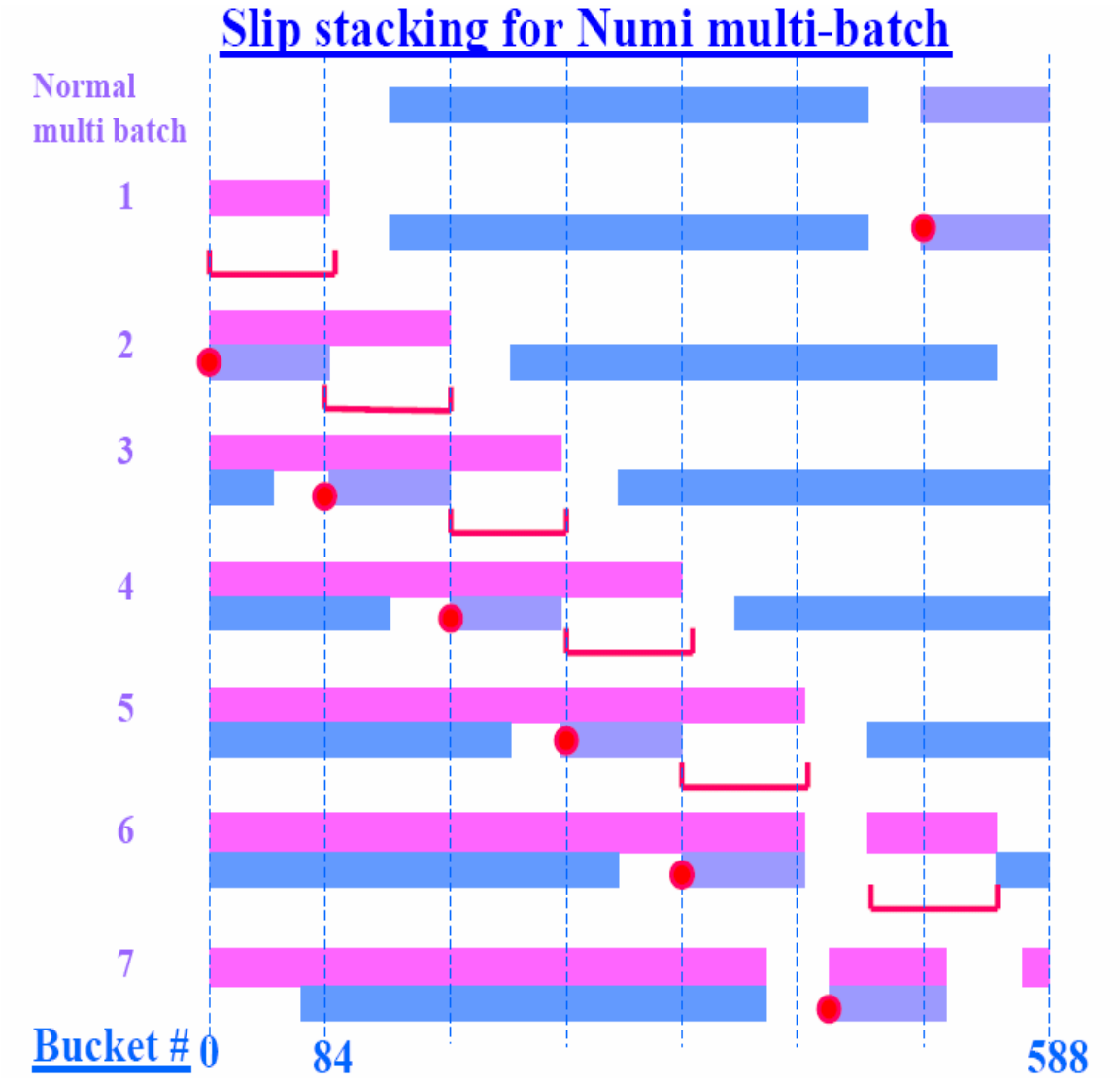

FIGURE 3.3.2: Cartoon illustrating the scheme for multi-batch slip-stacking. Four batches for NuMI (blue line) and one batch for pbar (cyan line) are first injected in the center of the MI aperture. This beam is decelerated by 1260Hz in one Booster tick and 6 more batches are injected (pink lines from 1 to 6). One more Booster tick is used to accelerate both species of beam around the center of the aperture and recapture (line 7). The red dots indicate the slippage of the first pbar batch with respect to revolution marker rotating with the center MI frequency.

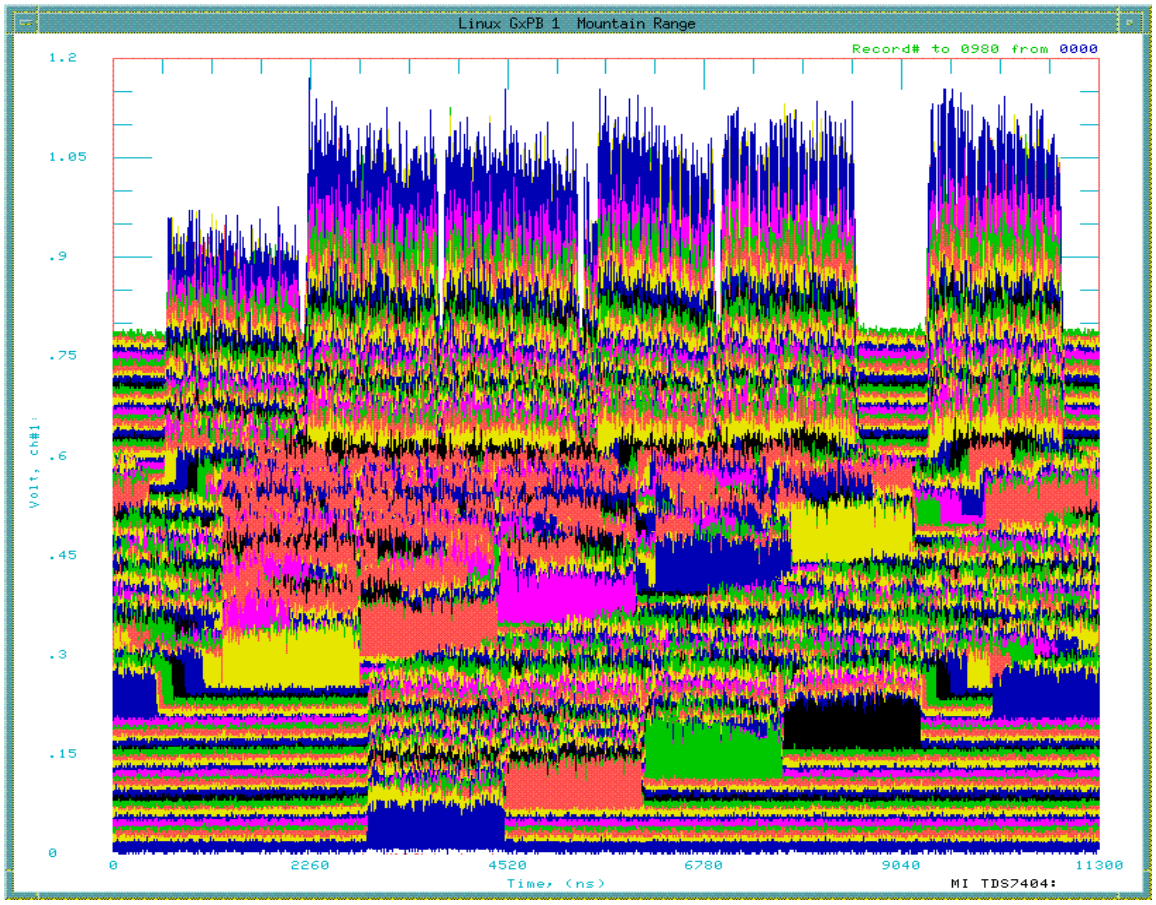

FIGURE 3.3.3: Mountain Range picture of multi-batch slip stacking in MI.

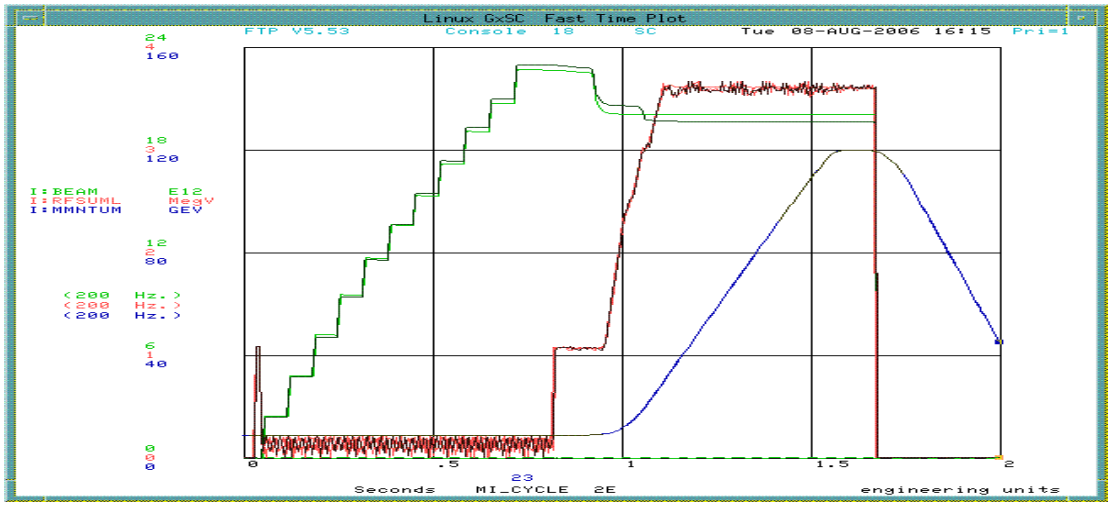

FIG 3.3.4: Beam Intensity (green), rf voltage (red) and energy (blue) during a multi-batch slip stacking cycle in MI. A total of 4E12 p have been accelerated to 120 GeV so far.

For the multi-batch slip stacking we assume that we will maintain the same level of beam loading compensation (14 db of fundamental feedback and 18 db of feed-forward). The sensitivity of slip stacking to the level of feed-forward gain is shown in Fig. 3.3.5.

The sensitivity of slip stacking to the momentum spread coming out of the Booster is shown in Fig. 3.3.6 where the percentage of the un-captured (DC Beam) generated during the multi-batch slip stacking is plotted as a function of the beam half momentum spread.

This WBS also includes a modest effort to explore RF barrier stacking for NuMI.

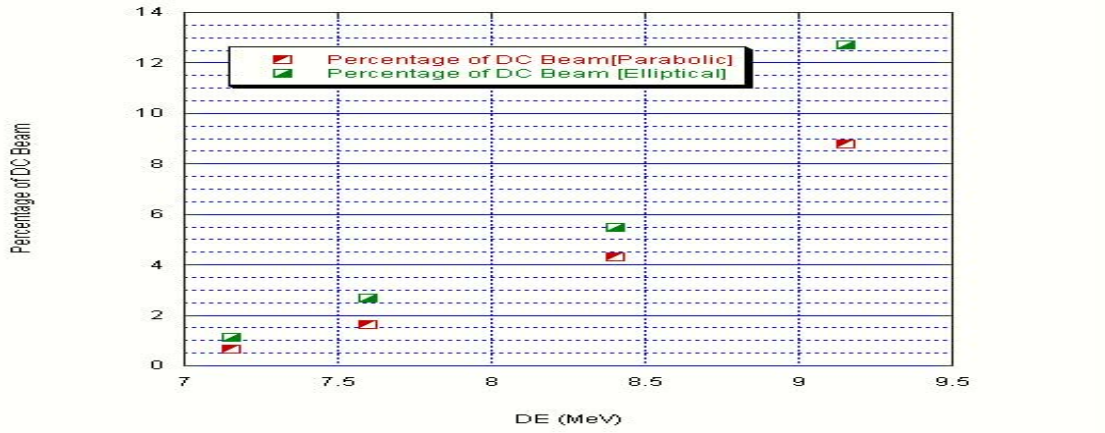

FIG 3.3.5: Sensitivity of slip stacking to the half momentum spread from Booster (ESME simulations). The percentage of DC beam produced during slip stacking is plotted vs. the half momentum spread of the beam.

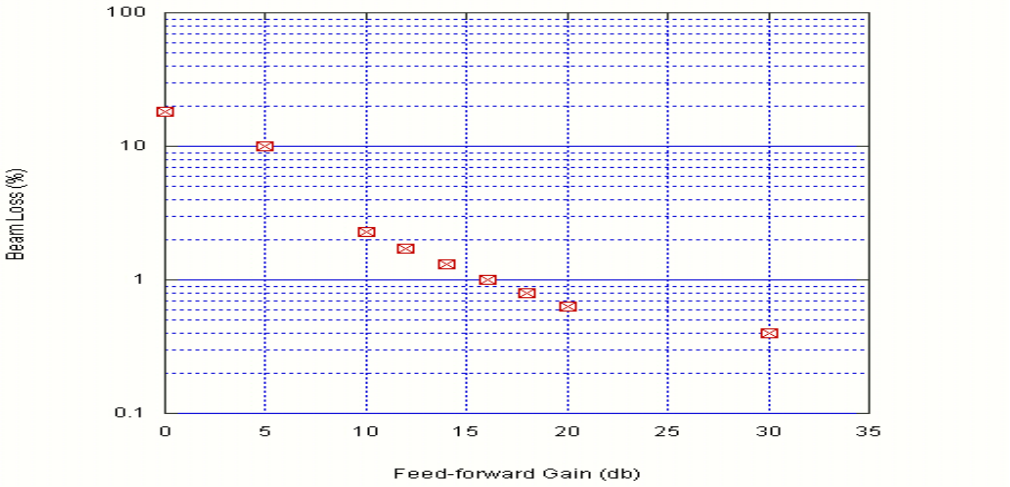

FIG 3.3.6: Sensitivity of slip stacking to the feed-forward compensation (ESME simulations). The percentage of beam loss is plotted vs. the feed forward compensation gain. In all these simulations a we assumed fundamental rf feed-back with a gain of 14 db.

WBS 1.3.3.2-Injection Kicker Modifications

MI-10 kicker had to be modified in order to be able to slip stack for NuMI. Originally the MI-10 kicker could be fired only up to 7 times every 2 sec mainly because of cooling reasons. For the Proton Plan the MI-10 kicker has to be able to fire with 15 Hz rate a total of 12 times in 2 sec. The cooling of the MI-10 kicker was changed from a convectively cooled system to a forced cooling system (100psi, 5gpm) with the installation of a flourinert cooling skid and upgraded loads. The cooling skid and the new loads along with an extensive array of piping were installed during the Spring 06 shutdown. A picture of the cooling skid is shown on Fig. 3.3.7 and a picture of the kicker waveform at the tail end before and after the cooling upgrade is shown of Fig. 3.3.8. From this last Figure we can see the reduction on the kicker tail and the improvement on the stability as the MI cycle time varied.

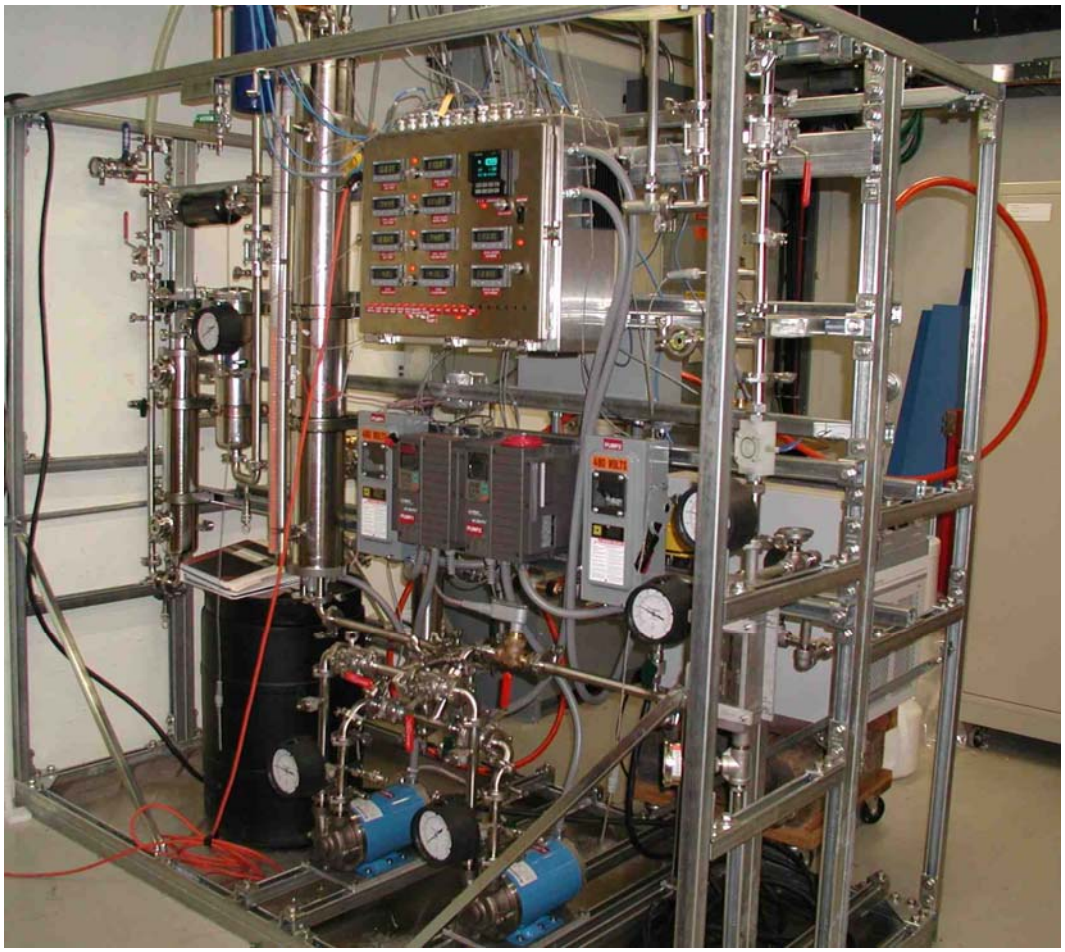

Fig. 3.3.7: Picture of the cooling skid for the MI-10 Kicker.

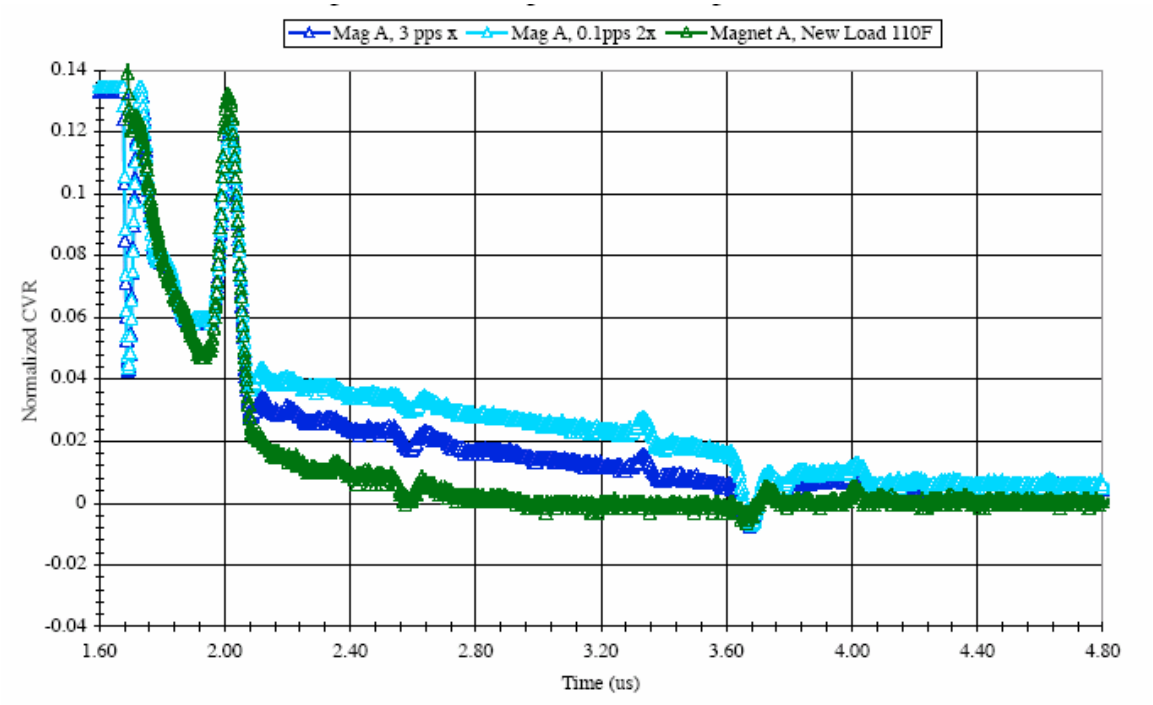

Fig. 3.3.8: Picture of the MI-10 Kicker tail wave form before(cyan, blue) and after the cooling upgrade (green).The two traces before the cooling upgrade correspond to two different running conditions. As we can see from the picture the kicker tail has been greatly reduced and the stability has improved.

WBS 1.3.3.3-Extraction Kicker Modifications

We plan to improve the MI-52 kicker after pulse in order to reduce the effect on the first NuMI batch. Currently we are observing an average of 1 mm transverse oscillation across the first NuMI batch after the pbar batch is kicked. The Image strip terminations were changed on both the MI-52 magnets without observing any significant improvement on the kicker after pulse. The next thing to try is to change the kicker loads in order to improve the matching. This will require making 4 new loads and installing them in the tunnel. A decision will be made soon if we proceed with this path.

WBS 1.3.4 – Main Injector RF Upgrade

H588 RF System Overview:

An overview of the existing MI h588 RF System is given in Table 3.4.1. Additional descriptions of the system are given in the text that follows.

Table 3.4.1: Overview of MI h588 RF System

Number of Cavities (Stations)	18
Number of Station Groups	2 (A/B)
Number of Stations per Group	9
Cavity Q	3000-5000
Cavity R/Q [1]	100
Cavity Tuning Range	52.55 - 53.5 MHz
Cavity Tuning Method	Ferrite Tuners
Single Cavity Accelerating Voltage Range	20 - 240 KV
Cavity RF Drive Source	Power Tetrode Tube (150kW anode dissipation) (Cathode Driven with 8kW Solid-State Amplifiers)
Individual Station Control Loops	Cavity Tuning
	Direct RF Feedback (variable gain 0 to ~25 V/V) [2] delay=~470nsec
	Local Station Phase Control
Station Group (A/B) Control Loops	MRF Magnitude (var gain 0 to 10, pole=100Hz)
	MRF Phase (var gain 0 to 10, pole = 20Hz)
Global Control Loops	LLRF Beam Phase Locked Loop
	LLRF Radial Position Loop
	Feed Forward Beam Loading Compensation (~15-18dB reduction at 1st revolution harmonics)
Beam Loading Compensation Methods	Direct RF Feedback
	Feed Forward
	Mode -1 longitudinal damper

[1] $R \equiv \frac{V^2}{2 \cdot P}$

[2] small signal gain

The MI h588 system consists of 18 High-Level RF (HLRF) cavity stations which are grouped as shown in Fig. 3.4.1. There are 3 Anode Power Supplies (APS) each of which powers 6 stations. The system is divided into two main groups: 9 Group A stations and 9 Group B stations. Each group is separately controlled in both amplitude and phase by the Low-Level RF (LLRF) and Mid-Level RF (MRF) control systems. The LLRF control system provides sequencer type control of RF vector manipulations along with a RF-to-beam phase-locked-loop and a beam radial position loop. The MRF control system is slaved to the LLRF and provides separate magnitude and phase regulation for each station group (A/B). This configuration permits the

creation of two accelerating voltage vectors at different frequencies for the slip-stacking process and allows 'paraphasing' (arbitrary vector addition) control of the vector sum.

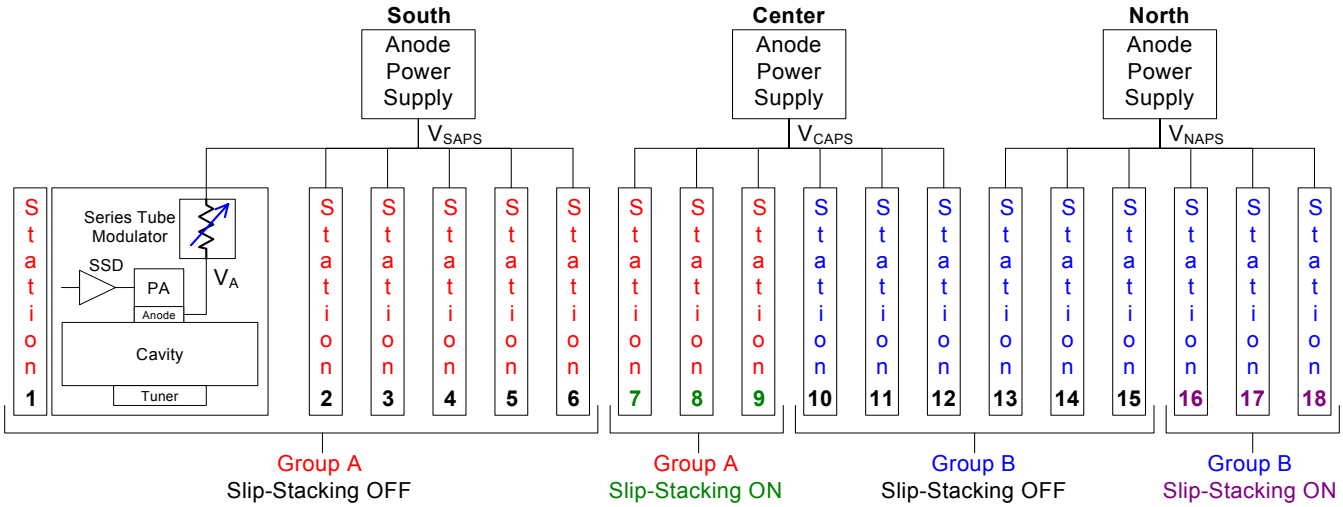

Figure 3.4.1: Present MI h588 RF system station configuration

Station ON/OFF gating is presently used to generate the low voltage required during slip-stacking. The 'Slip-Stacking ON' stations are those stations which are kept on during slipping to produce the slip-stacking RF voltage for their respective group. The 'Slip-Stacking OFF' stations are those stations whose LLRF drive is gated OFF in order not to contribute any RF voltage during slip-stacking; however, direct RF feedback and feed-forward beam loading compensation (BLC) are still active on these stations. This station on/off gating scheme is also used to create the necessary RF voltage for bunch rotation, which is still needed for pBar production. It is the individual cavity minimum and maximum operating voltages in combination with the requested slip-stacking and bunch rotation voltages which have dictated the number of Slip-Stacking ON/OFF stations.

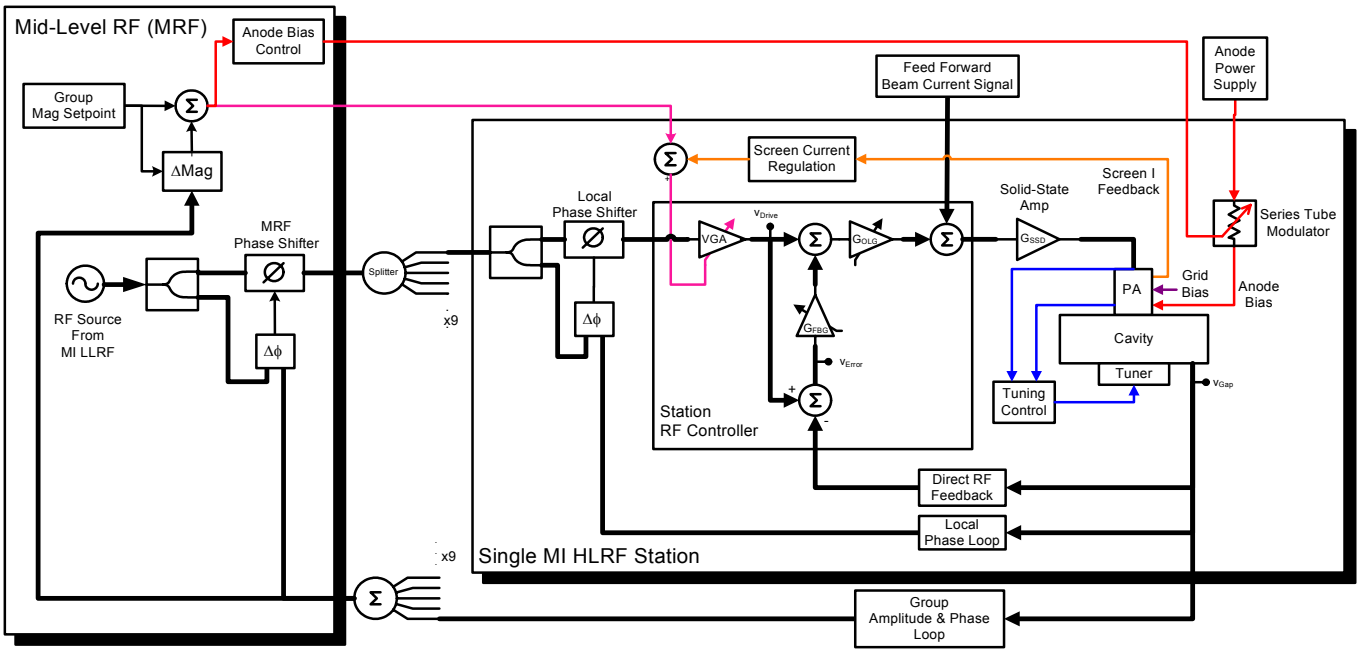

Figure 3.4.2: RF System block diagram showing individual station control loops and global MRF loops.

A block diagram view of an individual HLRF station and its associated control loops is shown with the global MRF loops in Figure 3.4.2. A group (A/B) magnitude set-point is translated by MRF into an individual station cavity voltage request and an appropriate power amplifier (PA) anode bias. The individual cavity voltage request is sent to a variable gain amplifier (VGA) which resides in the Station RF Controller. The VGA in turn provides the reference RF drive signal to the Direct RF Feedback (FB) loop which is configured as a 'drive+error' structure as shown. This 'drive+error' structure promotes a convenient calibration of the Direct RF FB loop. The 'drive+error' term proceeds to a variable gain amplifier which is referred to as an 'Open Loop Gain (OLG) Compensation' term that is meant to compensate for predictable changes in system gain due to frequency, PA biasing, and RF drive. The compensated RF drive signal is combined with the RF Feed Forward (FF) beam loading compensation (BLC) to ultimately become the RF generator current in the cavity via the solid-state drive (SSD) amplifiers and the RF PA. For a thorough description of the above architecture see Ref [3.4.1].

RF Cavities

Each cavity is tuned over the operating frequency range 52.8114-53.104 MHz, by two biased ferrite tuners inductively coupled symmetrically to the opposite lower cavity outer wall. The tuners and their coupling loops are water-cooled, as is the entire cavity (Fig. 3.4.4).

At present each cavity is driven by a single Eimac 4CW150000 power tetrode mounted directly on the cavity providing up to175 KW (operationally). Each cavity is designed to operate up to a maximum accelerating gap voltage of 240 KV at 53.104 MHz.

The cavity Q as a function of energy has been measured and is plotted in Fig. 3.4.3. The cavity Q is around 4800 for energies above transition. The effective shunt impedance is calculated from the cavity Q and the cavity geometric factor, $R_s / Q = 104$, to be $R_s = 5 \times 10^5 \Omega$.

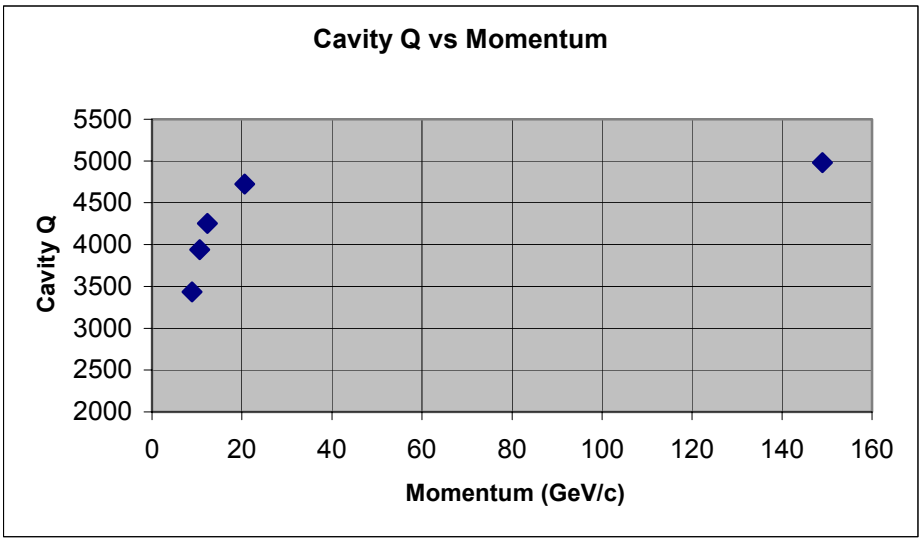

Fig. 3.4.3: Cavity Q vs. momentum.

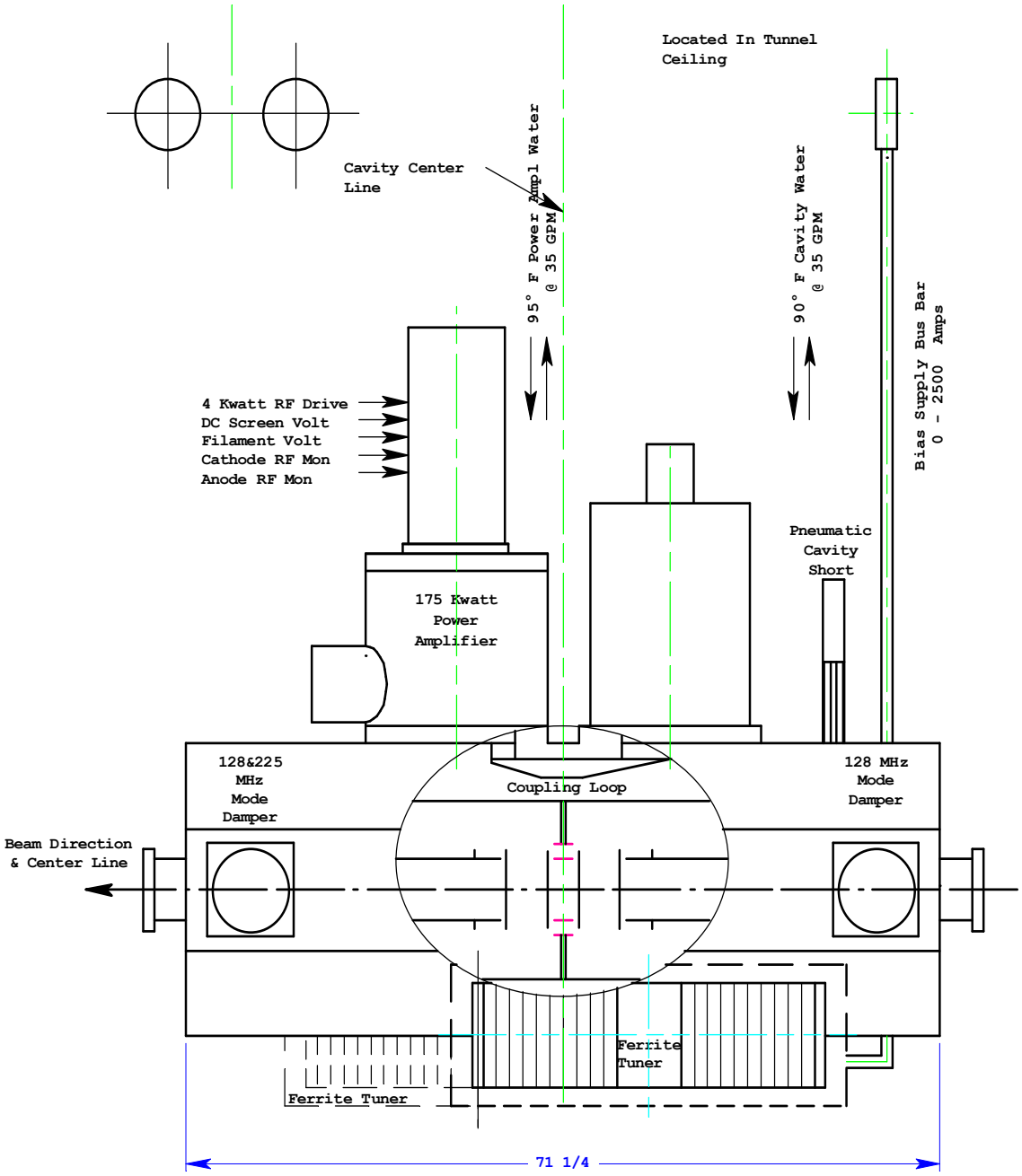

Present Main Injector Cavity

Fig. 3.4.4: Schematic of the present MI RF Cavity.

Beam Experiments

In the Main Injector we are using RF feedback around each station with typical gains of 6-10 [3.4.7]. Its effect is equivalent to introducing a shunt resistance across the accelerating gap, whose value is inversely proportional to the loop gain. In such a way the effective shunt resistance can be reduced by a large factor, increasing in proportion the beam current threshold.

In order to evaluate the effect of the RF feedback we measured how much we can reduce the RF voltage in a high intensity beam cycle without beam loss. In Fig. 3.4.5 we plot the beam intensity BEAM (green trace) along with the total RF voltage RFSUM (red trace) during a $2E MI cycle. In order to be able to reduce the RF voltage as much as possible no slip stacking was used in this cycle. We were unable to reduce the RF voltage much lower than 2.8 MV because the bucket area was getting too small (we were starting to see beam loss for a bucket area smaller than 0.75eV-sec). We can see in Figure 3.4.5 that we can accelerate up to 2.46E13 with 205 GeV/sec and 2.8 MV exceeding the Robinson stability limit by a factor of 1.84. Based on this result we can estimate that the number of protons that can be stably accelerated by the present RF system with 205 GeV/sec and 4.3 MV (240 KV per cavity) is 5.9E13.

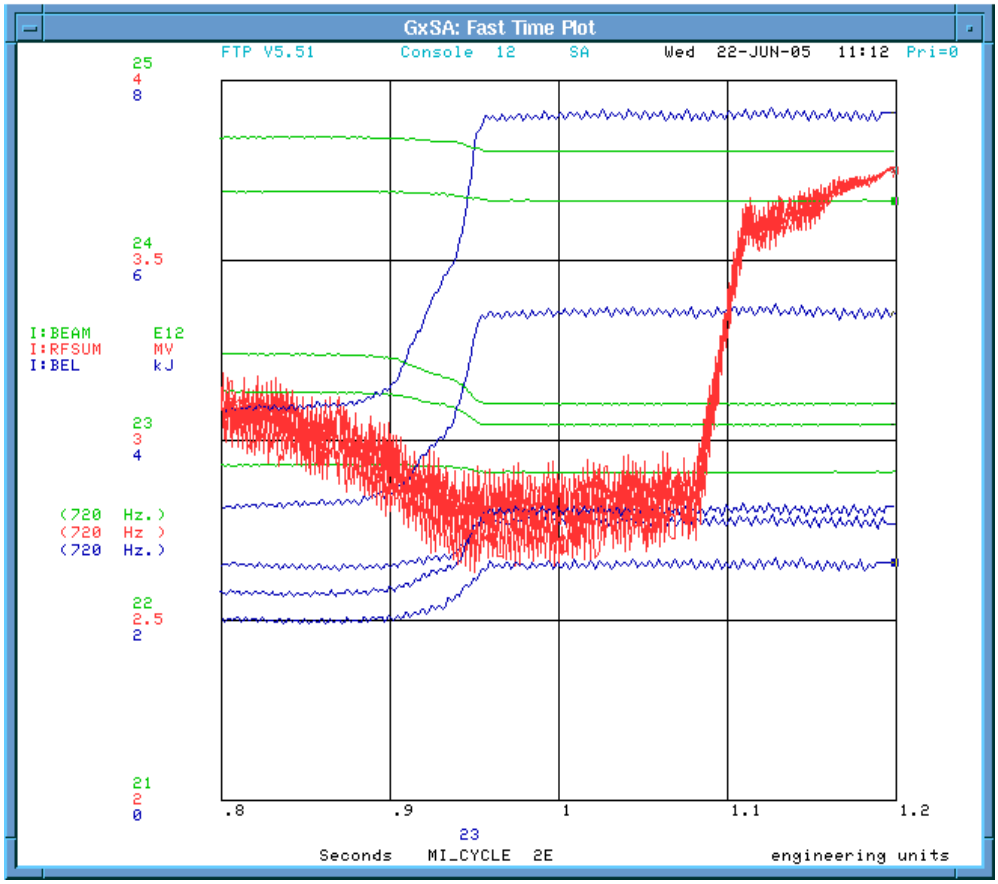

Fig. 3.4.5: Beam Intensity and RF voltage during a $2E MI cycle.

MI RF Issues

The Proton Plan presents the following generalized concerns for the MI h588 RF system:

1. The RF system has to support multi-batch slip-stacking at low RF voltage.
2. The total MI beam intensity is being increased ~40% from the previously achieved maximum intensity of ~3.2E13 to the Proton Plan goal of 4.5E13.

Slip-stacking is presently being used in daily operations for pBar production. Thus the RF system is already dealing with peak instantaneous beam loading similar to what is expected with multi-batch slip-stacking. However, the average power will increase and low-voltage operation (with heaviest beam-loading factor) will be extended from ~0.18 seconds to ~0.8 seconds.

The MI momentum ramp, bucket area, RF voltage, and beam synchronous phase angle for the multi-batch slip-stacking cycle are shown in Figs. 3.4.6 to 3.4.9 respectively.

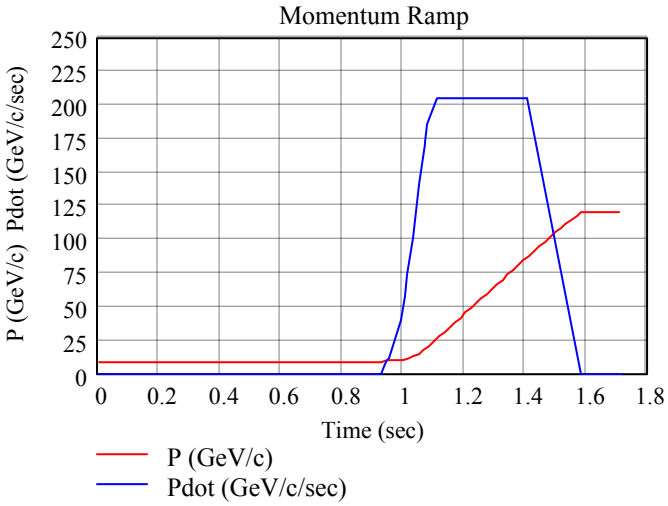

Figure 3.4.6: Multi-batch slip-stacking cycle momentum ramp

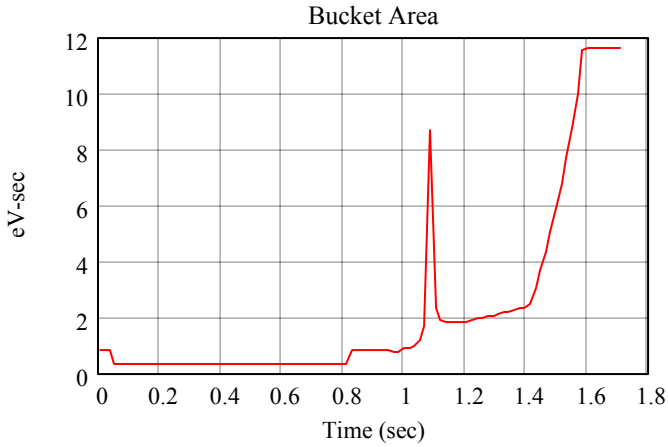

Figure 3.4.7: Multi-batch slip-stacking cycle bucket area

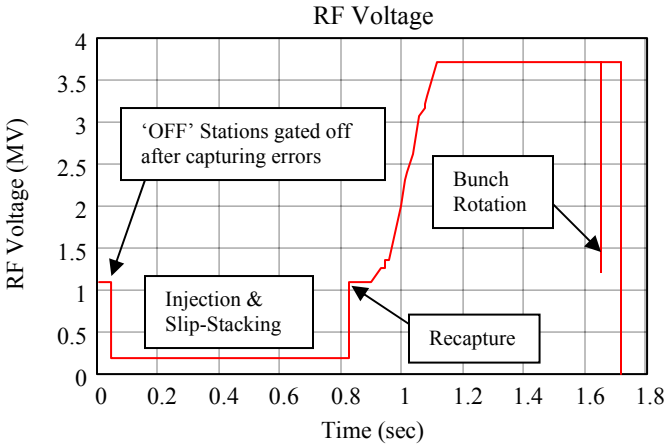

Figure 3.4.8: Multi-batch slip-stacking cycle RF Voltage profile.

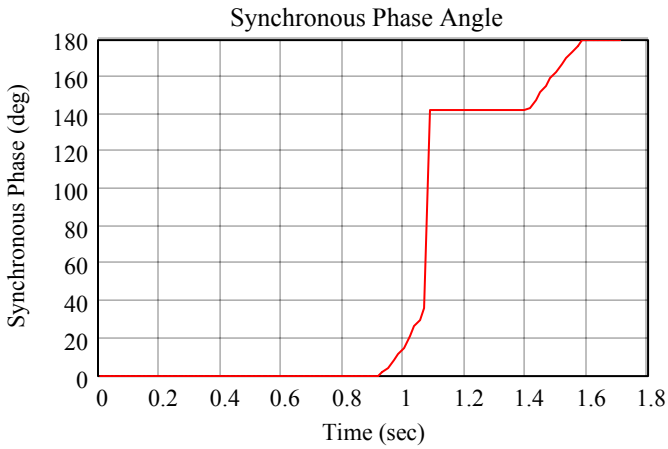

Figure 3.4.9: Beam synchronous phase angle; defined as the phase of the beam relative to the positive-slope zero crossing of the RF voltage.

The following issues have become evident for the MI RF System as a result of a power study (WBS 1.3.4.2.1):

1. The Series Tube Modulator power dissipation at injection
2. Two of three Anode Power Supply rectifier transformers need to be upgraded. See the 'Anode Power Supply (APS) Rectifier Transformers' section of this note.
3. The present 10kW SSD power supplies are presently underspecified for the ~55% efficient 8kW SSD amplifiers. See the 'SSD Power Supply' section of this note.

Series Tube Modulator (STM) Power Dissipation at Injection:

The STM modulator, as shown in Fig 3.4.2 is essentially a series resistor that drops the APS voltage in order to create the anode bias voltage for the RF PA. Thus when both the DC current and the STM voltage drop are large the STM power dissipation is large. This is exactly the situation that is presented with the multi-batch slip-stacking scenario and the historical MI RF station magnitude control method.

Historically, an RF station's magnitude control loop was based upon regulating the RF PA screen current. This meant that the DC anode bias had to be directly proportional to the desired cavity RF voltage. Thus, at low cavity RF voltage the PA anode bias also had to be low and the STM voltage drop had to be large. Since slip-stacking requires large PA DC anode current in order to generate almost perfect beam loading compensation at low cavity RF voltage, the STM power dissipation becomes an issue for multi-batch slip-stacking.

In fact it has been determined (Ref. [3.4.2] and [3.4.3]) that the required DC anode current will approach 6 to 8 amps at injection for the Slip-Stacking OFF stations. The requirements for the Slip-Stacking ON stations can be relaxed at injection by using half-detuning of the cavity (see Ref [3.4.2]). With the historic MI RF station magnitude control scheme, the PA DC anode bias is set to ~3.5 kV at injection. At an APS output voltage of 26kV this presents a voltage drop of ~22.5 kV across the STM. At 8 amps of DC anode current, the STM would have to dissipate 180kW; thus exceeding the rated plate dissipation of 150kW.

The solution to relaxing the STM power dissipation at injection is to use a true cavity voltage regulation scheme for RF station magnitude control. In this type of scheme the ultimate control of the RF drive is based upon the cavity RF voltage and not the PA tube screen current. Thus the PA anode can be biased higher (and the STM voltage drop lowered) while still maintaining the desired cavity RF voltage without drawing screen current. The conceptual difference in the historic screen current regulation method and the cavity voltage regulation scheme is depicted in Fig. 3.4.10.

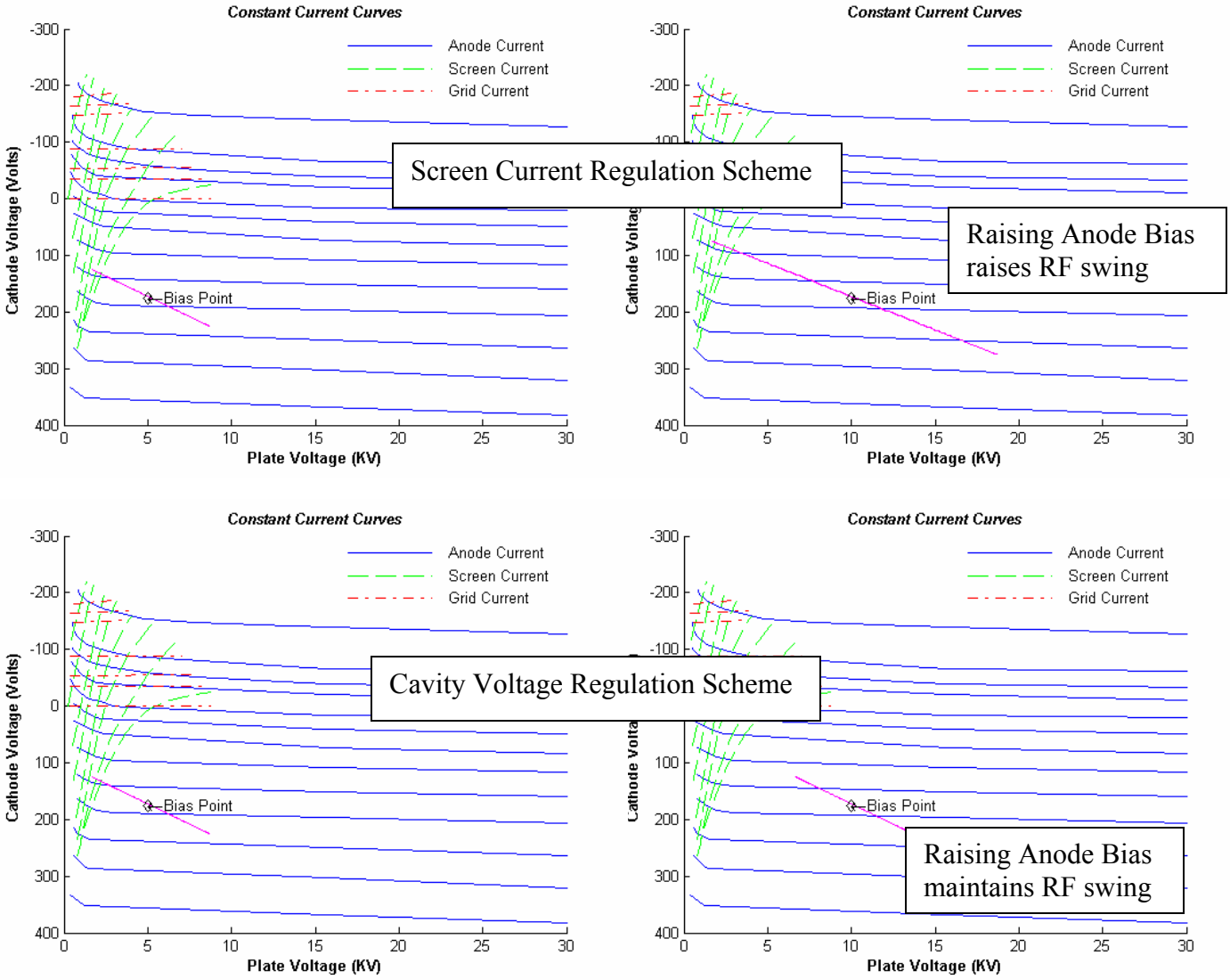

Figure 3.4.10: Conceptual difference between screen current regulation (top pictures) and cavity voltage regulation scheme (bottom pictures). The load line is shown in magenta. In the cavity voltage regulation scheme the anode voltage is not forced to swing into the screen current region.

Although the STM dissipation is relaxed by raising the anode bias along with true cavity voltage control, there is no real power savings since the APS output voltage is still the same and there is little to no change in the required DC anode current. What is achieved is better power balancing between the STM and the RF PA.

In order to implement true cavity voltage control and solve the STM power dissipation the following efforts are required:

- System Calibration with MRF (1.3.4.3)
- MI RF Sys Modulator Power Dissipation Resolution (1.3.4.4)

System Calibration with MRF (1.3.4.3)

The path to true cavity voltage control was paved with the introduction of Direct RF FB during the Run II slip-stacking upgrades and with the Mid-Level RF system (Ref. [3.4.5]). During the course of the Mid-Level RF upgrade provisions were made to address the series tube power dissipation issue for the Proton Plan with true cavity voltage control. The role of the screen current regulation module was minimized so that it acts only as a limiter and not as the ultimate RF station magnitude controller. Through this role reduction, the Direct RF FB could then become the final magnitude controller at the station level. Additionally, true global magnitude and phase control was introduced to replace the historic A/B balancing system.

Although provisions were made for the Proton Plan to take advantage of them, they were not fully implemented. WBS 1.3.4.3, 'MI RF Sys Calibration w/MRF' addressed this issue. The purpose of this WBS was twofold: (1) to properly calibrate the system since it had not had a thorough calibration since the installation of the Direct RF FB and the SSD upgrade, and (2) to prepare the system for using MRF to establish true cavity voltage control for addressing the STM power dissipation issue.

A proper calibration of the system was found to be needed because the various control loops in the system were not calibrated about the same 'zero error' condition (i.e. the zero error point of one loop did not correspond to zero error of the other loops). This led to large open loop errors which had to be brought into regulation by the outermost loops. Since pulling the system into regulation takes time, this produced unwanted transients in the system. During the spring 2006 shutdown, the opportunity to perform this calibration was presented. Examples of the positive results from the calibration are shown in Figs. 3.4.11 to 3.4.15.

For instance, Fig. 3.4.11 shows the improvement in the errors associated with the Direct RF FB loop at the station level as seen in the cavity voltage program signal and screen current regulation module. In the images, the 'Raw SSD Monitor' is the cavity voltage request coming from the MRF system (the Mag. Set-point of Fig. 3.4.2) and the 'Screen I Reg. Output Mon.' is the signal used to provide the RF reference to the Direct RF FB loop. Before the calibration, the 'OLG' compensation term of Fig. 3.4.2 was not being used. This caused the system gain to be too large towards the end of the cycle; thus causing excessive screen current and a large reduction of the 'Screen I Reg. Output Mon' signal. After the calibration, the Direct RF FB loop set-point ('Screen I Reg. Output Mon.') is seen to remain almost identical to the cavity voltage request ('Raw SSD Monitor'); thus indicating a substantial improvement in both open and closed loop errors and maintaining a direct proportionality between the requested cavity voltage and the actual cavity voltage.

Figure 3.4.12 shows the improvement in the Direct RF FB error (v_{Error} in Fig. 3.4.2) at the station level. The images are from a spectrum analyzer in zero-span frequency mode with a time-sweep covering a typical operational cycle. Improvements in both the open loop error ('Direct RF FB - ON' condition in image) and the closed loop error ('Direct RF FB – OFF' condition in image) are clearly seen.

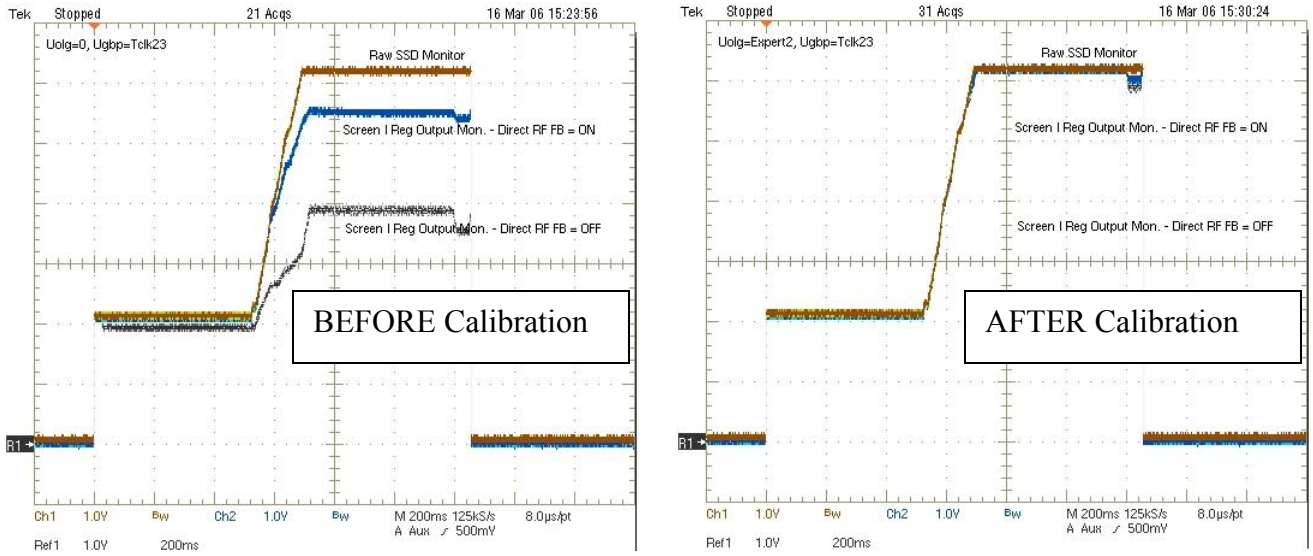

Figure 3.4.11: Demonstration of the improvements in the open and closed loop errors associated with the Direct RF FB loop at the station level as seen in the cavity voltage program signal. Left image is before the calibration, right image is after the calibration. See text for explanation.

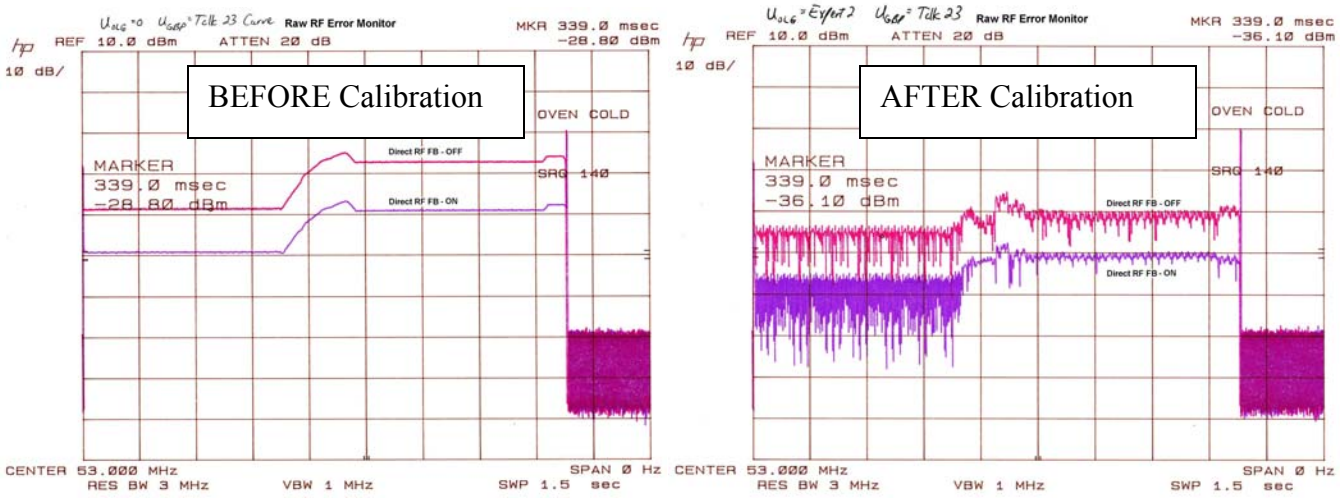

Figure 3.4.12: Demonstration of the improvements in the open and closed loop errors associated with the Direct RF FB loop at the station level as evidenced by the Direct RF FB error signal (v_{Error} of Fig. 3.4.2).

Finally, the images indicating that the overall purpose (system calibration and converting to true cavity voltage control) of the system calibration has been achieved are shown in Figs. 3.4.13 to 3.4.15.

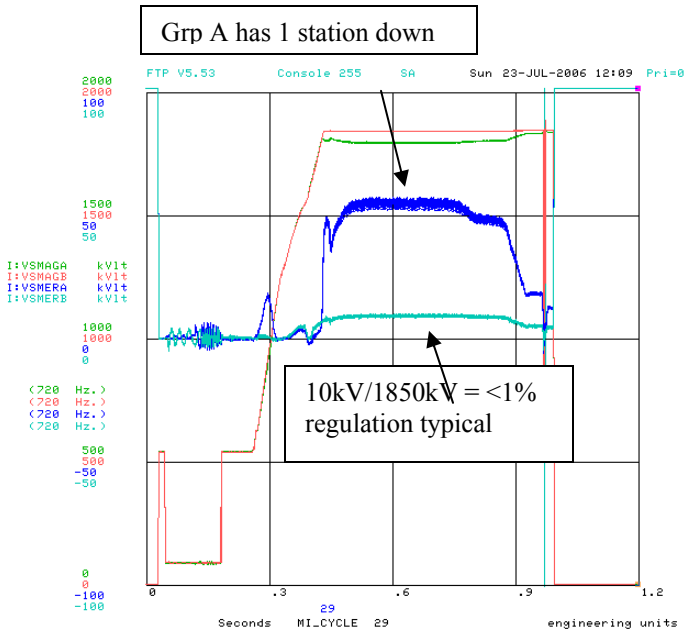

Figure 3.4.13: MRF Group (A/B) magnitude (I:VSMAGA/B) and magnitude errors (I:VSMERA/B) during a pBar slip-stacking cycle at ~7.5E12 total beam intensity. Note, Group A has 1 station down for this plot.

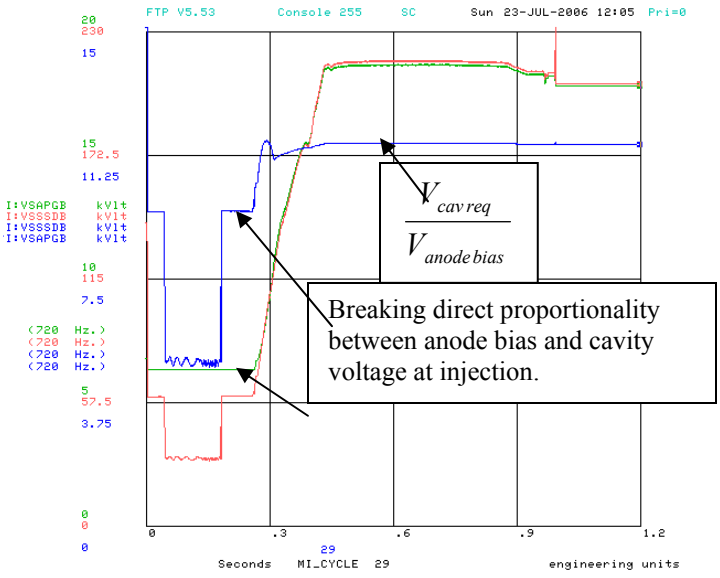

Figure 3.4.14: Proof of using higher anode bias at injection. True cavity voltage control without screen I regulation is possible. Note that the direct proportionality between the anode bias (I:VSAPGB) and the cavity voltage request (I:VSSSDB) is broken at injection.

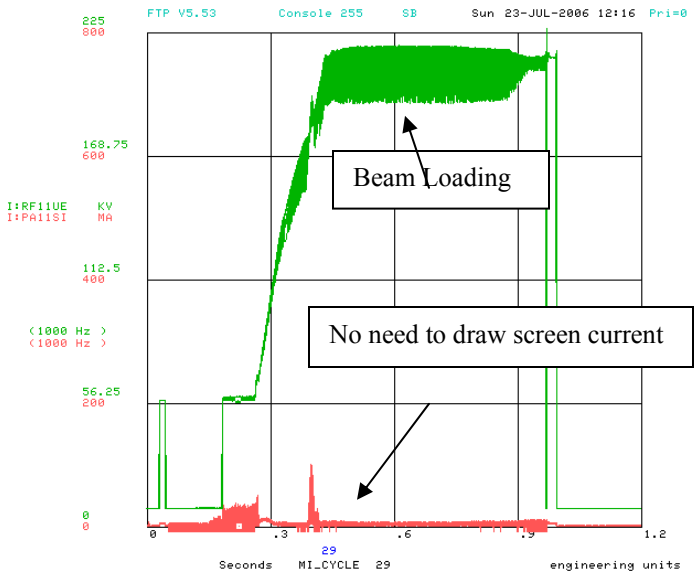

Figure 3.4.15: Proof of reducing the role of screen current regulation ; drawing screen current is not necessary.
I:RF11UE = detected cavity voltage at Stat. 11
I:PA11SI = PA screen current at Stat. 11

MI RF Sys Modulator Power Dissipation Resolution (1.3.4.4)

Calibrating the system with MRF only opens the door to solving the STM power dissipation issue. To implement the final anode bias level needed to relax the STM power dissipation:

1. The allowable anode bias level at injection needs to be investigated (1.3.4.4.1)
2. The final anode bias control scheme has to be implemented (1.3.4.4.2)

Cavity Tuner Voltage Limit Studies (1.3.4.4.1)

There are two constraints that dictate how high the PA anode bias can be raised. The first is the obvious constraint of not reversing the problem to an issue with the RF PA dissipation. The second is protection of the cavity tuners from RF sparking.

The Anode Limit Program (ALP) function has been a part of the MI RF system since the system's beginning. Its purpose is to protect the cavity tuners from RF sparking by limiting the PA anode bias and taking advantage of the natural saturation of the PA tube. Since the PA anode bias limits the RF swing of the anode, it also limits the RF voltage on the tuners. Historical experience found that a large enough RF voltage could be developed in the tuner that would cause destructive arcing.

ALP is a function of cavity resonant frequency due to the RF circuit behavior of the cavity/tuner geometry. Unfortunately, the value of ALP is lowest at injection. This is due to the tuners being inductive short-circuited stubs that are meant to resonant with the effective capacitance of the remainder of the cavity. Thus, the tuners exhibit their highest impedance at the lowest cavity resonant frequency.

The effect of ALP on the amount of beam intensity that is allowed without exceeding the STM power dissipation rating at injection has been explored in Ref [3.4.4]. A conservative estimate of the allowable beam intensity vs. ALP was calculated and is repeated here as Fig. 3.4.16.

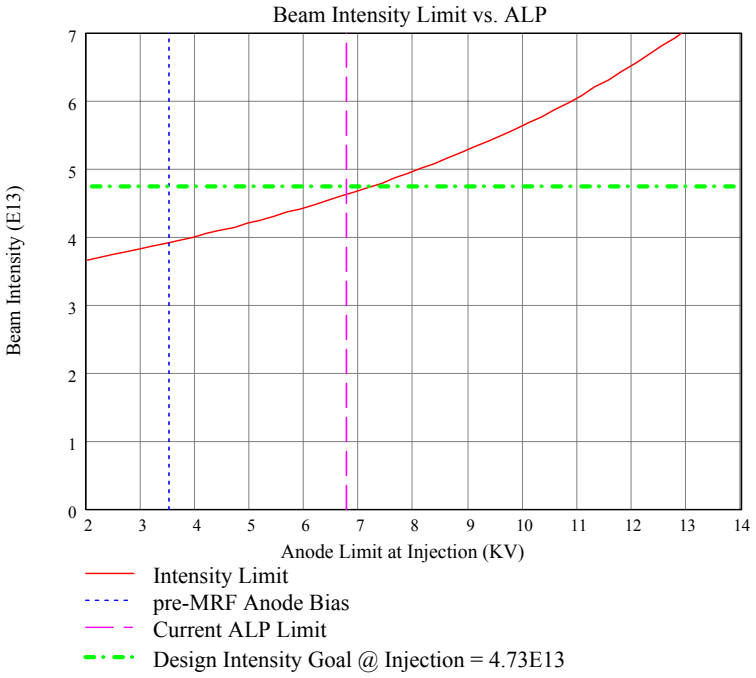

Figure 3.4.16: Beam intensity limit vs. ALP as limited by STM power dissipation at injection from Ref [3.4.4]. Assumptions: (1) 2xbunch form factor=2, (2) cavity gap:anode voltage ratio=12.25, (3) STM input voltage=26kV, (4) STM power dissipation limit = 135 kW, (5) 'moving average' formed from a single batch intensity.

From Fig. 3.4.16 it is clear that the historic screen current regulation scheme would substantially limit the allowed beam intensity. Even the present ALP limit of ~6.75 kV still limits the allowed beam intensity before exceeding STM power dissipation at injection. Thus, the question arises as to what is the proper ALP limit at injection that still protects the cavity tuners.

There is little historic evidence of what the actual cavity tuner RF voltage breakdown limit is. Reference [3.4.4] has begun to investigate the history of ALP and physical measurements on a test station cavity. As a result of this work it has been decided to comfortably raise ALP at injection to 9 kV. From Fig. 3.4.13, this raises the beam intensity limit to ~5.3E13 which is ~10% headroom. There is evidence that it can be raised even higher (Ref. [3.4.4]); however studies of the actual breakdown limit at the test station have to be completed before deciding on a higher limit and the possibility of requiring a new cavity tuner protection system that does not rely on the natural saturation of the PA tube.

Mid-Level RF Anode Control Design & Implementation (1.3.4.4.2)

Once the studies of 1.3.4.4.1 are complete and a final anode bias level at injection is chosen, it has to be implemented in the MRF control software. Initially it was thought that a software reconfiguration may be needed. However, there already exists a minimum anode program value which is part of the 'Anode Bias Control' block of Fig. 3.4.2. This minimum value can easily be changed within software to reflect the final choice for the ALP value at injection. Additional effort will be required to retune the 'APG A/B Overdrive' watchdog protection modules. These modules offer global protection from the anode bias program being driven over the ALP function. This effort is estimated to be minimal since it only requires retuning within an existing module.

MI RF Cavity Protection System (1.3.4.5)

A new cavity tuner protection system (WBS 1.3.4.5.1) would be needed if the final value of PA anode bias required at injection does not still provide protection to the cavity tuners via the natural saturation of the PA tube. This tuner protection system would most likely be in the form of a RF probe directly near the tuners which constantly monitors the tuner RF voltage and interlocks the station if the tuner voltage exceeds a predetermined protection level; as opposed to a photo-multiplier tube (PMT) spark detection system as originally proposed.

Originally it was estimated that a calorimetry system (1.3.4.5.2) would benefit power measurements and possibly offer a means to protect the STM and RF PA tubes from excessive power dissipation. Since RF PA power dissipation is not an issue (Ref [3.4.2]) calorimetry was not pursued on the RF PA. Furthermore, since faster $V \cdot I$ protection (WBS 1.3.4.5.4) was designed, calorimetry also was not pursued for the STM's. The $V \cdot I$ protection has been designed to monitor the STM power dissipation and interlock the station if the power dissipation exceeds a conservative threshold. The installation of these modules is complete.

It has been observed that the Direct RF FB loop can go unstable if a station is attempted to be turned on during the middle of an operational cycle. This is due to the fact that phase margin in the Direct RF FB loop is lost if the ferrite tuner control loses lock and the cavity is completely

detuned. Modifications to the station Modulator External Interlock Control Unit (MEICU) are necessary to prevent turning a station on mid-cycle (WBS 1.3.4.5.3).

Beam Loading Compensation System Upgrades (1.3.4.6)

Feed Forward System Improvements (1.3.4.6.1)

Since Feed Forward (FF) beam loading compensation is such a critical component to proper beam loading compensation, the present FF system is being investigated to identify areas of improvement. The intent is to minimize the error between the FF system's output signal and the beam current signal (which is its input signal).

Currently, there are unnecessary spectral components that are present in the FF signal as evidenced in Figs. 3.4.17 and 3.4.18. Figure 3.4.17 is a time domain plot of the FF signal. The beam is clearly seen as the two large pulses. The noise in between the pulses has been found to be due to LO leakage from the down-convert/up-convert process used to generate the one-turn delay. Figure 3.4.18 is the corresponding frequency domain representation of the same signal as measured with a spectrum analyzer. Notated on the picture are the LO frequency at 49 MHz and the unwanted cross products.

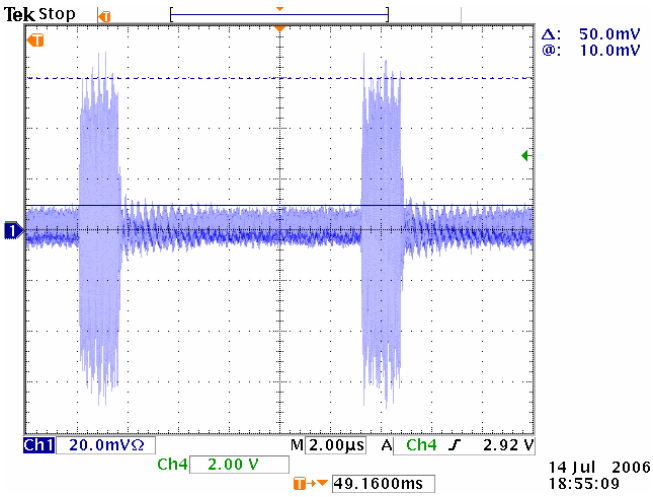

Figure 3.4.17: Time domain measurement of the present Feed Forward signal.

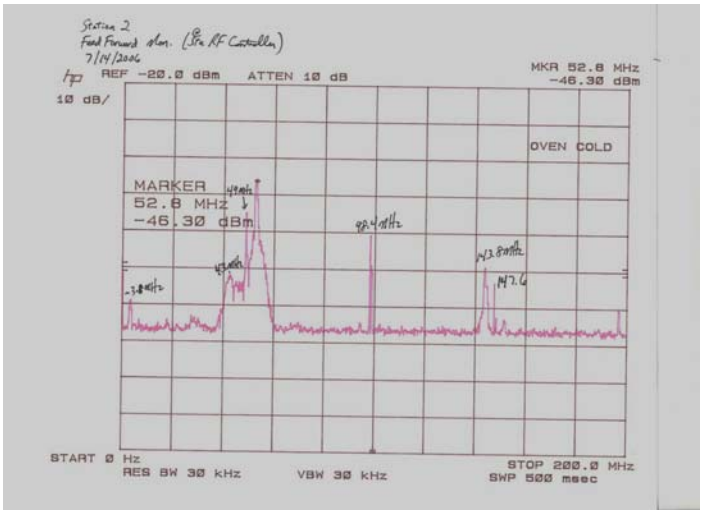

Figure 3.4.18: Frequency domain measurement of the present Feed Forward signal.

The following areas have been identified for improvement:

- The intermediate frequency (IF) path
  - A different IF frequency will be explored along with optimized filtering in the IF path to minimize IF leakage and unwanted cross products
- Add a band-pass filter to the output.
  - Currently there is no band-pass filter on the output of the system, thus unwanted frequency components are present in the FF signal which is delivered to each

station. These unwanted signals can cause problems at the station level (i.e. waste real power in the PA and interfere with the operation of phase detectors).

Cavity Tuning Controller Upgrade (1.3.4.6.2)

Studies from WBS 1.3.3 have revealed the following:

- The overwhelming source of emittance dilution for slip-stacked batches is the interaction of the slipping buckets during the slip stacking process with our present 14dB of direct RF feedback and ~18dB of Feed Forward.

- If the cavity de-tuning is limited to 65 degrees, the longitudinal coupled bunch modes should be kept stable or readily controlled with the existing Mode -1 longitudinal damper (Ref [3.4.6]). The longitudinal coupled bunch mode growth rates normalized to the landau frequency spread from Ref. [3.4.6] is repeated here as Fig. 3.4.19.

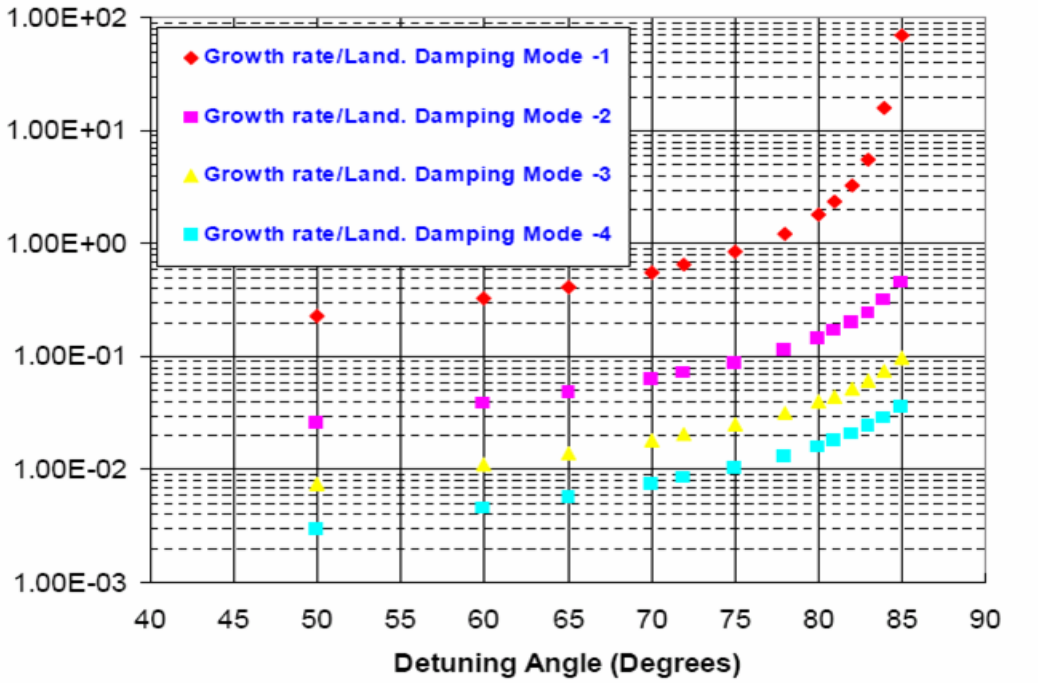

Figure 3.4.19: Longitudinal coupled bunch mode growth rates vs. cavity detuning angle from Ref. [3.4.6].

Presently there is no phase offset adjustment in the cavity tuning control system; thus we do not have complete control over the cavity de-tuning angle. Adding this level of control will require an upgrade to the present analog cavity tuning controllers to a more sophisticated digital cavity tuning controller. A prototype will have to be developed and tested at both the MI-60 test station and in an operational station. This prototype will be developed using existing digital technology that has been developed for longitudinal dampers at the lab. It is estimated to take ~6 months to develop a prototype and finalize the design and another 6 months to mass produce and install the final design for all 18 HLRF stations.

Anode Power Supply (APS) Rectifier Transformers

During the course of the studies of Ref [3.4.2] and [3.4.4] the following issues with the APS rectifier transformers became evident:

- The Center APS rectifier transformer's lowest tap setting can only reduce the APS output voltage to ~30 kV unloaded (~28 kV loaded). This causes two problems:
  - Even at the increased ALP value of 9kV, the STM voltage drop on the center stations would still be too high to allow the design intensity goal. The beam intensity limit for 28kV STM input voltage and ALP=9kV is found from Fig. 3.4.13 (at ALP equal to 7kV since the plot assumes 26kV STM input) to be less than the design intensity goal.
  - There would be little headroom between the expected peak power requirement from the Center APS and its rated maximum instantaneous specification of 2400 KVA. See Ref [3.4.2].

- The South APS rectifier transformer is the oldest (>25 years old) of the rectifier transformers. While the expected average power requirement from the South APS is expected (Ref. [3.4.2]) to be below the 1700 KVA thermal rating of the South APS rectifier transformer, little is known about its instantaneous maximum rating. The transformer is the same style as that used in Booster for which its output reaches 2800 KVA for 5msec. Ref [3.4.2] estimates that the South APS will have to provide ~2000 KVA for greater than 0.2 sec. and a peak of ~2200 KVA for ~40 msec. The concensus within the RF Department is that the South APS rectifier transformer is not guaranteed to meet the specifications. Thus it will be upgraded.

The following upgrade path has been decided for the APS rectifier transformers:

- The North APS rectifier transformer will be left alone. It is the newest of the three with a 2000 KVA thermal rating and a 2800 KVA maximum instantaneous rating. These specifications are well above the expected requirements (Ref [3.4.2]).
- The Center APS rectifier transformer will be replaced with a spare transformer that is on-site. This spare transformer is of the same style as the North APS rectifier transformer which meets expected requirements and provides a ~25 kV loaded output voltage; thus it will not present a problem with the STM power dissipation.
- The South APS rectifier transformer will be upgraded.
- A total of 2 new rectifier transformers will be purchased. One to replace the South APS rectifier transformer and one as a spare. A specification for the transformers will be sent out for quote. It is estimated to take ~1 year to receive the transformers.

SSD Power Supply

The present 10kW SSD power supplies are presently underspecified for the ~55% efficient 8kW SSD amplifiers. This is not an issue for present operations; however the average SSD forward power requirements are expected to increase for Proton Plan. It is estimated that average forward power can approach ~4kW (Ref [3.4.2]). Furthermore, transients may require us to have

the full 8kW available. The SSD power supplies should be replaced with a 15kW version. The infrastructure of the 480V AC distribution is sized to handle the 15kW version.

References:

[3.4.1] T.Berenc, P.Varghese, P.Joireman, B.Barnes, B.Chase, J.Dey, J.Reid, "The Mid-Level RF (MRF) Handbook", Fermilab RF TechNote TN#076, Dec. 2005.
< http://www-rfes.fnal.gov/global/technotes/TN/TN076.pdf>

[3.4.2] T.Berenc, I.Kourbanis, D.McGinnis, J.Reid, "Main Injector RF Power Requirement Calculations for the Proton Plan", Fermilab beams-doc #2311, June 2006.
< http://beamdocs.fnal.gov/AD-public/DocDB/ShowDocument?docid=2311>

[3.4.3] T.Berenc "Main Injector HLRF Measurements for Proton Plan", Fermilab beams-doc #2331, July 2006.
< http://beamdocs.fnal.gov/AD-public/DocDB/ShowDocument?docid=2331>

[3.4.4] T.Berenc, J.Reid "Main Injector HLRF Anode Limit Program & Cavity Tuner RF Voltage Limit", Fermilab beams-doc #2317, June 2006.
< http://beamdocs.fnal.gov/AD-public/DocDB/ShowDocument?docid=2317>

[3.4.5] T.Berenc, B.Chase, R.Pasquinelli, J.Reid "A Brief History of the MI 53MHz RF System Run II Upgrades", Fermilab RF TechNote TN#073, Sept. 2005.
< http://www-rfes.fnal.gov/global/technotes/TN/TN073.pdf>

[3.4.6] I.Kourbanis, "Growth Rates of Coupled Bunch Modes due to the Fundamental RF Impedance", Fermilab beamd-doc #2379, July 2006.
< http://beamdocs.fnal.gov/AD-public/DocDB/ShowDocument?docid=2379>

[3.4.7] J.Dey, J. Steimel, J. Reid, "Narrowband Beam Loading Compensation in The Fermilab Main Injector Accelerating Cavities", PAC2001, Chicago, IL, June 18-11 2001, p.876.